

# Correlated theory of triplet photoinduced absorption in phenylene-vinylene chains

Alok Shukla

*Physics Department, Indian Institute of Technology, Powai, Mumbai 400076, India*

(Received 15 August 2001; revised manuscript received 5 December 2001; published 11 March 2002)

In this paper, the results of large-scale correlated calculations of the triplet photoinduced-absorption (PA) spectrum of oligomers of poly-(para)phenylenevinylene (PPV) containing up to five phenyl rings are presented. In particular, the high-energy features in the triplet PA spectrum of oligo-PPV's are the focus of this study, which, to our knowledge, have not been investigated theoretically or experimentally. The calculations were performed using the Pariser-Parr-Pople model Hamiltonian and many-body effects were taken into account by means of the multireference singles-doubles configuration-interaction procedure without neglecting any molecular orbitals. The computed triplet PA spectrum of oligo-PPV's exhibits rich structure consisting of alternating peaks of high and low intensities. The predicted higher-energy features of the triplet spectrum can be tested in future experiments. Additionally, theoretical estimates of exciton binding energy are also presented.

DOI: 10.1103/PhysRevB.65.125204

PACS number(s): 71.20.Rv, 71.35.-y, 78.30.Jw

## I. INTRODUCTION

Photoluminescent conjugated polymer poly-(para)phenylenevinylene (PPV) is one of the most promising candidates for the optoelectronic devices of the next generation, such as light-emitting diodes<sup>1</sup> and lasers.<sup>2</sup> Because of their quasi-one-dimensional character, the electrons ( $e$ ) and holes ( $h$ ) in conjugated polymers have a high recombination probability, leading to their large photoluminescence (PL) efficiency.<sup>1</sup> However, in electroluminescence experiments, a significant fraction of the  $e$ - $h$  recombination events lead to the formation of triplet excitons, which are nonluminescent.<sup>3</sup> In addition, it is believed that through various other processes such as intersystem crossing<sup>4</sup> and fission,<sup>5</sup> the singlet excitons in these materials transform into the triplet ones. Therefore, in order to fully characterize the PL properties of conjugated polymers such as PPV, a thorough understanding of their triplet excited states is required. A good understanding of the triplet states is fruitful from another vantage point as well. The energy difference between the triplet and singlet states defines the exchange energy, and consequently, quantifies the strength of  $e$ - $e$  correlations in the system. Therefore, a deeper understanding of the triplet states will also enhance our understanding of electron-correlation effects in conjugated polymers. Recently Österbacka *et al.*,<sup>4</sup> Romanovskii *et al.*,<sup>6</sup> and Monkman *et al.*<sup>7</sup> have measured the energies of the first singlet ( $S_1$ ) and triplet ( $T_1$ ) excited states of various conjugated polymers. Triplet excited states with energies higher than  $T_1$  are frequently probed through the photoinduced-absorption (PA) spectroscopy in the triplet manifold.<sup>5,4</sup> In these experiments first the  $T_1$  is populated, and then the optical transitions are induced to higher-energy triplet states. Assuming a planar configuration for oligo-PPV's corresponding to symmetry group  $C_{2h}$ , their one- and two-photon states will belong, respectively, to the  $B_u$  and  $A_g$  irreducible representations. The ground state of these oligomers is  $1^1A_g$ , while  $S_1$  corresponds to  $1^1B_u$ . In the triplet manifold,  $T_1$  corresponds to the  $1^3B_u$  state, while the first state with a strong dipole coupling to  $1^3B_u$  is called  $m^3A_g$ .

Therefore, in the triplet PA spectrum of oligo-PPV's,  $m^3A_g$  would show up as the first peak, while any higher  $^3A_g$ -type states with significant dipole coupling to  $1^3B_u$  would lead to high-energy features in the spectrum. Therefore, through triplet PA spectroscopy, one can probe the triplet two-photon states ( $^3A_g$ ) of oligo-PPV's. However, so far all the theoretical,<sup>8-10</sup> and experimental<sup>4,5</sup> investigations of triplet PA in PPV's have focused on the first  $m^3A_g$  state, providing no information on the higher-energy  $^3A_g$ -type states. Considering recent PA measurements of high-energy two-photon states in the singlet manifold ( $^1A_g$ ) of the PPV's, which have yielded a lot of exciting information on the nature of those states,<sup>11</sup> we believe that a similar analysis should be extended to the high-energy  $^3A_g$ -type states of this material. Therefore, to fill that void, we decided to undertake a systematic large-scale correlated calculation of the triplet PA spectrum of oligo-PPV's that will target the high-energy features at the same level of computational accuracy as the  $m^3A_g$  peak. However, compared to the singlet- $A_g$  manifold responsible for the singlet PA, the correlation effects are stronger in the triplet- $A_g$  manifold because here, in addition to the orbital excitations, spin excitations are also involved. Therefore, it is mandatory that the correlated calculations employ large basis sets in order to describe the high-energy  $^3A_g$  peaks accurately. In absence of any prior calculations of this kind, for the purpose of benchmarking we also performed calculations on a number of other excited states of oligo-PPV's, and compared them to the works of other authors. As a matter of fact, our calculations on the triplet PA spectrum indicate the existence of three peaks beyond  $m^3A_g$  exhibiting a rich structure with alternating high and low intensities. We hope that this paper will encourage experimental measurements of the high-energy region in the triplet PA spectrum of PPV's, just as in similar recent measurements of their singlet PA spectrum.<sup>11</sup>

The remainder of this paper is organized as follows. In Sec. II we briefly describe the correlation approaches used to perform the calculations in the present paper. Next, in Sec. III, we present and discuss the calculated triplet PA spectrum

TABLE I. For different states of various oligomers, the number of reference configurations ( $N_{ref}$ ) and the total number of configurations ( $N_{total}$ ) involved in the MRSDCI (or QCI, where indicated) calculations.

Oligomer	$1^1A_g$		$1^1B_u$		$1^3B_u$		$m^3A_g$	
	$N_{ref}$	$N_{total}$	$N_{ref}$	$N_{total}$	$N_{ref}$	$N_{total}$	$N_{ref}$	$N_{total}$
PPV-2	1 <sup>a</sup>	49495	1 <sup>a</sup>	82423	1 <sup>a</sup>	144543	72	112193
PPV-3	1 <sup>a</sup>	2003907	1 <sup>a</sup>	3416371	65	1212746	65	1321885
PPV-4	35	1627923	36	1503239	35	2136547	35	2766111
PPV-5	25	3257930	25	2537197	25	3217908	20	3314575

<sup>a</sup>QCI method.

of oligo-PPV's. Finally, in Sec. IV we summarize our conclusions and discuss possible directions for future work.

## II. METHODOLOGY

Henceforth, any oligomer of PPV containing  $n$  phenyl rings will be referred to as PPV- $n$ , making *trans*-stilbene synonymous with PPV-2. We performed correlated calculations on the oligomers PPV-2 to PPV-5, assuming completely planar geometries and the symmetry group  $C_{2h}$ . From among a variety of model Hamiltonians available,<sup>9</sup> we chose the Pariser-Parr-Pople (PPP) model for the present calculations, which describes the  $\pi$ -electron dynamics of conjugated systems in terms of a minimal basis set, and a small number of parameters. The PPP Hamiltonian reads

$$H = - \sum_{\langle ij \rangle, \sigma} t_{ij} (c_{i\sigma}^\dagger c_{j\sigma} + c_{j\sigma}^\dagger c_{i\sigma}) + U \sum_i n_{i\uparrow} n_{i\downarrow} + \sum_{i < j} V_{ij} (n_i - 1)(n_j - 1), \quad (1)$$

where  $\langle ij \rangle$  implies nearest neighbors,  $c_{i\sigma}^\dagger$  creates an electron of spin  $\sigma$  on the  $p_z$  orbital of carbon atom  $i$ ,  $n_{i\sigma} = c_{i\sigma}^\dagger c_{i\sigma}$  is the number of electrons with spin  $\sigma$ , and  $n_i = \sum_\sigma n_{i\sigma}$  is the total number of electrons on atom  $i$ . The parameters  $U$  and  $V_{ij}$  are the on-site and long-range Coulomb interactions, respectively, while  $t_{ij}$  is the nearest-neighbor one-electron hopping-matrix element. The Coulomb interactions are parametrized as per the Ohno relationship<sup>12</sup>

$$V_{i,j} = U / \{ \kappa_{i,j} (1 + 0.6117 R_{i,j}^2)^{1/2} \}, \quad (2)$$

where  $R_{i,j}$  is the distance (in Å) between the sites  $i$  and  $j$ , and  $\kappa_{i,j}$  is the dielectric constant to account for screening. Since the results obtained with the PPP Hamiltonian depend substantially on the choice of the Coulomb parameters, we tried two sets: (a) "standard parameters" with  $U = 11.13$  eV and  $\kappa_{i,j} = 1.0$  and (b) "screened parameters" with  $U = 8.0$  eV and  $\kappa_{i,i} = 1.0$  and  $\kappa_{i,j} = 2.0$  with  $i \neq j$ . The screened parameters, originally introduced by Chandross and Mazumdar<sup>8</sup> in their study of optical absorption in PPV, are known to give better agreement with experiments on excitation energies, possibly by taking interchain screening effects into account. For the nearest-neighbor hopping-matrix elements  $t_{ij}$ , we chose  $-2.4$  eV for the phenylene ring, and  $-2.2$  eV and  $-2.6$  eV, respectively, for the single and double bonds of the vinylene linkage. As far as the bond

lengths are concerned, in the phenyl rings they were taken to be 1.4 Å. In the vinylene linkage the single (double) bond lengths were taken to be 1.54 Å (1.33 Å).

Starting with the restricted Hartree-Fock (HF), depending on the size of the oligomer, the electron-correlation effects were included either by the quadruple configuration-interaction (QCI) method or by the multireference singles-doubles configuration-interaction (MRSDCI) approach. Both the approaches are well documented in the literature.<sup>13</sup> The accuracy of the MRSDCI calculations depends on the choice of the reference configurations, and their number ( $N_{ref}$ ). The reference configurations are chosen according to their contribution to the many-particle wave function of the targeted state, while the convergence of our results with respect to  $N_{ref}$  will be examined in the following section. To reduce the size of the Hamiltonian matrices, we made full use of the spin and the  $C_{2h}$  point-group symmetry. The triplet PA spectrum was calculated using the oscillator strengths computed under the electric-dipole approximation. The finite lifetime of the states was taken into account by means of a linewidth parameter  $\Gamma$ . Further technical details can be found in our recent paper, where we used this symmetry-adapted CI methodology to study the low-lying excited states in phenyl-substituted polyacetylenes.<sup>14</sup>

## III. RESULTS AND DISCUSSION

The correlation method,  $N_{ref}$ , and the total number of configurations,  $N_{total}$ , involved in the CI calculations of excited states of various oligo-PPV's are detailed in Table I. From the sizes of the CI matrices diagonalized it is clear that these calculations were very large scale, and therefore, they must include the influence of electron-correlation effects to a very high accuracy. The convergence of our MRSDCI results with respect to  $N_{ref}$  is demonstrated in Fig. 1. It is clear from the results that good convergence in the excited-state energies has been achieved in all the cases by the time 15 most important configurations ( $N_{ref} = 15$ ) have been included in the reference space in various MRSDCI calculations, leading us to believe that the excitation energies presented here are accurate to within a few hundredths of an eV, for the given values of PPP parameters.

The noteworthy aspect of the present calculations as compared to those of other authors<sup>9,10,15</sup> is that no molecular orbitals have been discarded from the correlated calculations. Lavrentiev *et al.*,<sup>10</sup> with the purpose of obtaining results for infinite PPV, performed density-matrix renormalization-

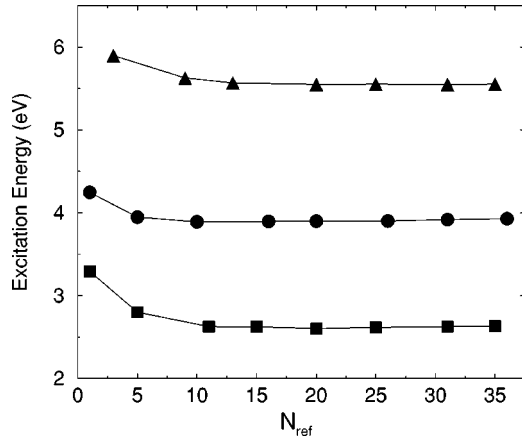


FIG. 1. Behavior of  $1^3B_u$  (squares),  $1^1B_u$  (circles), and  $m^3A_g$  (triangles) excited states of PPV-4 with respect to the number of reference configurations ( $N_{ref}$ ) included in the MRSDCI calculations performed with standard parameters.

group calculations in conjunction with a PPP-Hamiltonian-based two-state model consisting of just the highest occupied and the lowest unoccupied MOs (HOMO and LUMO) of each phenylene and vinylene unit. Thus, e.g., for PPV-5, which has 38 MO's in total, the number of active MO's considered by Lavrentiev *et al.*<sup>10</sup> was just 18. Additionally, Lavrentiev *et al.*<sup>10</sup> used a different set of PPP parameters as compared to us. Similarly Gartstein *et al.*<sup>15</sup> simplified the PPP model to obtain analytical results for the energy of  $1^3B_u$  state, but only for infinite PPV. Rohlfling and Louie<sup>16</sup> performed first-principles calculations on both the singlet and triplet states of infinite PPV. Beljonne *et al.*<sup>9</sup> performed calculations on the same oligomers of PPV as considered by us, utilizing an intermediate neglect of differential overlap

model Hamiltonian, also within the framework of the MRSDCI procedure. However, they used only four reference configurations ( $N_{ref}=4$ ), and considered single and double excitations from a set of five highest occupied  $\pi$  orbitals into the five lowest unoccupied  $\pi^*$  orbitals.<sup>10</sup> Thus,  $N_{ref}$  as well as the number of active MO's used by Beljonne *et al.*<sup>9</sup> is much smaller compared to our calculations. Therefore, to benchmark our computational approach and the choice of PPP Coulomb parameters, we compare our MRSDCI results on various low-lying excited states of  $PPV-n$  ( $n=2-5$ ) to those of other authors and experiments in Table II.

Inspection of Table II reveals the following trends.

(i) Our MRSDCI excitation energies computed with the screened Coulomb parameters are lower, and in better agreement with the experiments, than those computed with the standard parameters.

(ii) For  $E(1^3B_u)$  our calculations predict complete saturation, in excellent qualitative agreement with the highly localized picture of the  $1^3B_u$  state verified recently in the experiment of Österbacka *et al.*,<sup>4</sup> reporting that  $1^3B_u$  was a Frenkel exciton, with a radius of just 3.2 Å. However, neither our calculations, nor those of other authors are close to the experimental value of  $E(1^3B_u) \approx 1.5$  eV for the infinite PPV.<sup>4,7</sup>

(iii) As far as comparison with other authors is concerned, our screened parameter values of  $E(1^1B_u)$  are in similar agreement with the experiments as those of Beljonne *et al.*,<sup>9</sup> while they are somewhat higher than those of Lavrentiev *et al.*<sup>10</sup> whose  $E(1^1B_u)$  for PPV-5 is lower than the experimental value. However, our screened parameter values of  $E(m^3A_g) - E(1^3B_u)$  are consistently in much better agreement with experiments as compared to those of Beljonne *et al.*<sup>9</sup> and Lavrentiev *et al.*<sup>10</sup> This is very encouraging because, in order to compute the triplet PA spectrum accurately,

TABLE II. Comparison of our results with the standard parameters (this work 1) and screened parameters (this work 2) with those of other authors and experiments. All the energies are in eV.

	Work	PPV-2	PPV-3	PPV-4	PPV-5
$1^1A_g-1^1B_u$	This work 1	4.48	4.11	3.93	3.83
	This work 2	4.34	3.91	3.65	3.46
	Beljonne <i>et al.</i> (Ref. 9)	4.48	3.88	3.53	3.47
	Lavrentiev <i>et al.</i> (Ref. 10)	4.17	3.52	3.18	2.99
	Exp.	3.71 <sup>a</sup>	3.43 <sup>b</sup>	3.20 <sup>b</sup>	3.07 <sup>b</sup>
$1^1A_g-1^3B_u$	This work 1	2.66	2.64	2.63	2.62
	This work 2	2.20	2.19	2.22	2.21
	Beljonne <i>et al.</i> (Ref. 9)	2.73	2.52	2.44	2.63
	Lavrentiev <i>et al.</i> (Ref. 10)	2.65	2.16	1.95	1.84
$1^3B_u-m^3A_g$	This work 1	3.74	3.16	2.92	2.90
	This work 2	3.25	2.55	2.14	1.93
	Beljonne <i>et al.</i> (Ref. 9)	4.15	3.26	2.75	2.46
	Lavrentiev <i>et al.</i> (Ref. 10)	3.63	3.04	2.61	2.34
	Expt.	3.29 <sup>c</sup>	2.30 <sup>d</sup>	1.95 <sup>d</sup>	1.80 <sup>d</sup>

<sup>a</sup>Reference 17.

<sup>b</sup>Reference 18.

<sup>c</sup>Reference 19.

<sup>d</sup>Reference 5.

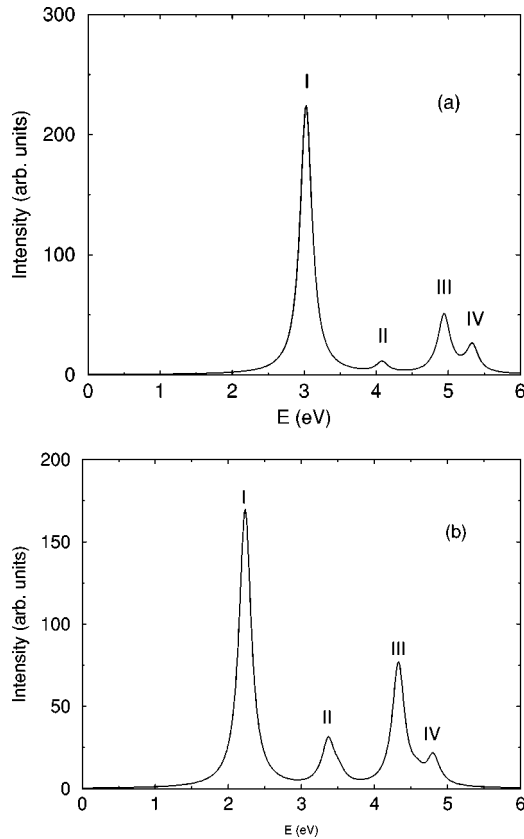


FIG. 2. Photoinduced absorption spectrum from  $1^3B_u$  state in PPV-4: (a) computed with the standard parameters; (b) computed with the screened parameters. A linewidth parameter  $\Gamma=0.1$  eV was used.  $E$  is the energy of the incident photon.

one needs to have an accurate representation of states in the  $^3A_g$  manifold, starting with the  $m^3A_g$  state.

To further benchmark our approach, we use  $E(m^3A_g)$  computed above to obtain a theoretical estimate of the binding energy of the  $1^1B_u$  exciton. Shimoi and Mazumdar have argued that, because  $m^3A_g$  state is also an exciton,  $E(m^3A_g) - E(1^1B_u)$  is a good lower-limit estimate  $E_b(\text{min})$  for the exciton binding energy.<sup>20</sup> From our calculations, for PPV-5 one gets  $E_b(\text{min})=0.68(1.7)$  eV with screened (standard) parameters. Keeping in mind that generally our screened-parameter-based calculations were in good agreement with the experiments, we take the value  $E_b(\text{min})=0.68$  eV to be the correct theoretical estimate. Thus our theoretical estimate of  $E_b(\text{min})=0.68$  eV obtained from PPV-5 is in very good agreement with the experimental value of  $E_b(\text{min})=0.55$  eV estimated by Österbacka *et al.*<sup>4</sup> for infinite PPV.

Next we turn our attention to the main focus of this paper—the triplet PA spectrum of oligo-PPV's. The calculated spectrum of PPV-4 is presented in Fig. 2, and of PPV-5 in Fig. 3. The spectra have been computed both with the standard parameters [Figs. 2(a) and 3(a)], as well as with the screened parameters [Figs. 2(b) and 3(b)]. Thus, the four presented spectra will help us understand the influence of the following two factors on the triplet PA: (i) the conjugation length and (ii) the strength of Coulomb interactions.

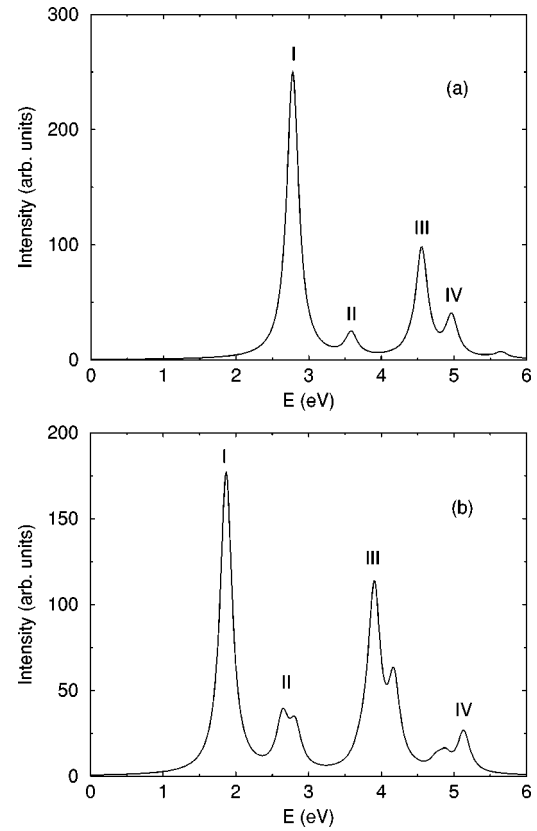


FIG. 3. Photoinduced absorption spectrum from  $1^3B_u$  state in PPV-5: (a) computed with the standard parameters; (b) computed with the screened parameters. A linewidth parameter  $\Gamma=0.1$  eV was used.  $E$  is the energy of the incident photon.

The following trends emerge from the spectra presented in Figs. 2 and 3: (i) Irrespective of the Coulomb parameters used, both for PPV-4 and PPV-5 there are four major structures (labeled I, II, III, and IV) of alternating high and low intensities; (ii) Irrespective of the Coulomb parameters, the relative intensities of the high-energy peaks (II, III, and IV), as compared to peak I, are increasing with increasing conjugation length; (iii) For a given oligomer, the relative intensities of the high-energy peaks, compared to peak I, are higher when computed using screened parameters, as compared to those calculated using the standard parameters. Although, standard-parameter-based calculations yield rather small relative intensities for peaks II of PPV-4 and PPV-5, however, the same parameters lead to significant intensities of other high-energy peaks (III and IV). Thus, based upon these results, we arrive at the following conclusions regarding triplet PA in oligo-PPV's.

(i) The intensities of peak III and beyond are strong enough to be detected experimentally in rather small oligomers such as PPV-4 and PPV-5.

(ii) The intensity of peak II for small oligomers appears to be strongly dependent on the strength of Coulomb interactions. This peak will be detectable for these oligomers only if screened parameters, perhaps due to interchain screening, describe the strength of Coulomb interactions.

(iii) For relatively longer oligomers, even peak II will acquire significant intensity both for standard and screened



parameters, as exemplified by the rapid increase in its intensity with size.

Having discussed the general qualitative features of the computed triplet PA spectrum, we next examine the nature of many-particle  ${}^3A_g$  states contributing to various peaks. Here we limit our discussion to the specific case of the spectrum of PPV-5 computed with screened parameters as presented in Fig. 3(b). The reasons behind this choice are obvious—PPV-5 is the longest oligomer studied, and the values of the energy gaps  $E(m{}^3A_g) - E(1{}^3B_u)$  with screened parameters for various oligomers were in very good agreement with the experiments. However, we did examine the nature of the peaks in the triplet spectra presented in the remaining three figures [Figs. 2(a), 2(b), and 3(a)], and all of them were found to be qualitatively very similar to the states corresponding to the peaks in Fig. 3(b). Thus we believe that our discussion of triplet PA spectrum of PPV-5, computed with screened parameters, represents the general features of the triplet PA spectra of oligo-PPV's. The first peak in Fig. 3(b), occurring close to 1.9 eV, is the strongest in the spectrum, and corresponds to the  $1{}^3B_u \rightarrow m{}^3A_g$  absorption. Compared to the Hartree-Fock configuration, the many-particle wave function of  $m{}^3A_g$  is a linear combination consisting mainly of singly excited configurations ( $H-1 \rightarrow L$ ) and its charge-conjugated (c.c.) counterpart ( $H \rightarrow L+1$ ), where  $H$  denotes HOMO and  $L$  denotes LUMO. Feature II located near 2.7 eV has a smaller intensity compared to I, and corresponds to two closely spaced  ${}^3A_g$  states also consisting predominantly of single excitations ( $H \rightarrow L+3$ ) + c.c. and ( $H-1 \rightarrow L+2$ ) + c.c. The intensity of the next feature (III) is much stronger compared to that of II, and is composed of states with main contributions from *double excitations*. The dominant peak of III, located near 3.9 eV, corresponds to a  ${}^3A_g$  state composed predominantly of double excitation ( $H-1 \rightarrow L; H \rightarrow L+1$ ). Feature IV has weaker intensity compared to III, and its main peak occurs close to 5.1 eV. Similar to III, this feature also corresponds to states composed of doubly excited configurations. The state constituting the main peak of IV is predominantly composed of ( $H \rightarrow L+2; H-2 \rightarrow L$ ) and other double excitations. In the infinite-polymer limit, we speculate that the single-excitation-based features I and II will merge to form the first absorption band, while the double-excitation-based features III and IV would merge to form the second band. Thus, for infinite PPV, we expect the triplet PA spectrum to be similar in appearance to its singlet counterpart, which also exhibits two major bands PA1 and PA2.<sup>21</sup>

Experimental measurement of triplet PA peaks beyond  $m{}^3A_g$  (peak I) is not an easy task.<sup>22</sup> However, if it is possible

to conquer the associated practical difficulties, we believe that the measurements of the high-energy region of the triplet PA will shed light on some important excited states of PPV, thereby further clarifying the role of electron-correlation effects in this substance.

#### IV. CONCLUSIONS AND FUTURE DIRECTIONS

In conclusion, very large-scale correlated calculations using the PPP Hamiltonian were performed on oligo-PPV's, and their triplet PA spectrum extending well into the high-energy region was computed. The computed spectrum predicts rich structure beyond  $m{}^3A_g$ , consisting of peaks with alternating high and low intensities. The peaks were shown to result from  ${}^3A_g$ -type states composed predominantly of configurations, which, besides the spin excitation, also exhibit either single or double charge excitations with respect to the ground state. Therefore, it will be interesting to probe the higher-energy triplet PA spectrum, both of oligomers as well as of infinite PPV experimentally, as it will lead to further insights into the low-lying excited states of this technologically important material. Analogous to the singlet manifold, it will then also be of interest to explore the existence of triplet biexcitons.

Although the electron-correlation effects were included up to a large accuracy in the present calculations, yet, because of the use of a rigid-lattice model, the influence of electron-lattice coupling was completely ignored. However, recently Barford *et al.*<sup>23</sup> have demonstrated that the contribution of electron-lattice relaxation can be important on the low-lying correlated triplet states. They demonstrated that for polyenes,  $1{}^3B_u$  state can relax by a few tenths of an eV thereby increasing the corresponding  $E(m{}^3A_g) - E(1{}^3B_u)$  energy gap.<sup>23</sup> Therefore, it will be of considerable interest to perform a similar calculation for oligo-PPV's, and compute the contribution of electron-phonon coupling on the triplet excitation energies of these materials. These aspects as well as phosphorescence and triplet electroluminescence in conjugated polymers will be studied theoretically shortly.

#### ACKNOWLEDGMENTS

The author is grateful to S. Mazumdar for a critical reading of the manuscript and for numerous suggestions for improvement. A part of this work was performed at the Max-Planck-Institut für Physik Komplexer Systeme (MPIPKS), Dresden, Germany. These calculations were performed on the Alpha workstations of the Physics Department, IIT, Bombay, and MPIPKS.

<sup>1</sup>R.H. Friend, R.W. Gymer, A.B. Holmes, J.H. Burroughes, R.N. Marks, C. Taliani, D.D.C. Bradley, D.A. Dos Santos, J.L. Bredas, M. Logdlund, and W.R. Salaneck, *Nature (London)* **397**, 121 (1999).

<sup>2</sup>N. Tessler, G.J. Denton, and R.H. Friend, *Nature (London)* **382**, 695 (1996).

<sup>3</sup>See, e.g., M. Wohlgenannt, K. Tandon, S. Mazumdar, S. Ramase-

sha, and Z.V. Vardeny, *Nature (London)* **409**, 494 (2001), and references therein. These authors showed both theoretically and experimentally that during the *e-h* recombination events in conjugated polymers, the cross section for singlet formation is significantly larger than that for the triplet formation, thus increasing the fraction of singlets formed significantly above the statistical limit of 25%. However, still the fraction of triplet ex-

- citons formed during  $e$ - $h$  recombination events is quite significant.
- <sup>4</sup>R. Österbacka, M. Wohlgennant, D. Chinn, and Z.V. Vardeny, *Phys. Rev. B* **60**, R11 253 (1999).
- <sup>5</sup>G. Cerullo, G. Lanzani, S. De Silvestri, H.-J. Egelhaaf, L. Lüer, and D. Oelkrug, *Phys. Rev. B* **62**, 2429 (2000).
- <sup>6</sup>Yu.V. Romanovskii, A. Gerhard, B. Schweitzer, U. Scherf, R.I. Personov, and H. Bässler, *Phys. Rev. Lett.* **84**, 1027 (2000).
- <sup>7</sup>A.P. Monkman, H.D. Burrows, L.J. Hartwell, L.E. Horsburgh, I. Hamblett, and S. Navaratnam, *Phys. Rev. Lett.* **86**, 1358 (2001).
- <sup>8</sup>M. Chandross and S. Mazumdar, *Phys. Rev. B* **55**, 1497 (1997).
- <sup>9</sup>D. Beljonne, Z. Shuai, R.H. Friend, and J.L. Brédas, *J. Chem. Phys.* **102**, 2042 (1995).
- <sup>10</sup>M.Yu. Lavrentiev, W. Barford, S.J. Martin, H. Daly, and R.J. Bursill, *Phys. Rev. B* **59**, 9987 (1999).
- <sup>11</sup>S.V. Frolov, Z. Bao, M. Wohlgenannt, and Z.V. Vardeny, *Phys. Rev. Lett.* **85**, 2196 (2000).
- <sup>12</sup>K. Ohno, *Theor. Chim. Acta* **2**, 219 (1964).
- <sup>13</sup>See, e.g., P. Tavan and K. Schulten, *Phys. Rev. B* **36**, 4337 (1987).
- <sup>14</sup>H. Ghosh, A. Shukla, and S. Mazumdar, *Phys. Rev. B* **62**, 12 763 (2000).
- <sup>15</sup>Yu.N. Gartstein, M.J. Rice, and E.M. Conwell, *Phys. Rev. B* **52**, 1683 (1995).
- <sup>16</sup>M. Rohlfiing and S.G. Louie, *Phys. Rev. Lett.* **82**, 1959 (1999).
- <sup>17</sup>R.H. Dyck and D.S. McClure, *J. Chem. Phys.* **36**, 2326 (1962).
- <sup>18</sup>G.H. Gelinck, J.J. Piet, B.R. Wegewijs, K. Müllen, J. Wildeman, G. Hadziioannou, and J.M. Warman, *Phys. Rev. B* **62**, 1489 (2000).
- <sup>19</sup>W.G. Herkstroeter and D.S. McClure, *J. Am. Chem. Soc.* **90**, 4522 (1968).
- <sup>20</sup>Y. Shimoi and S. Mazumdar, *Synth. Met.* **85**, 1027 (1997).
- <sup>21</sup>S.V. Frolov, M. Liess, P.A. Lane, W. Gellermann, Z.V. Vardeny, M. Ozaki, and K. Yoshino, *Phys. Rev. Lett.* **78**, 4285 (1997).
- <sup>22</sup>Z.V. Vardeny (private communication).
- <sup>23</sup>W. Barford, R.J. Bursill, and M.Yu. Lavrentiev, *Phys. Rev. B* **63**, 195108 (2001).